7-2011

Stability Analysis and Application of a Mathematical Cholera Model

Shu Liao

Jim Wang
Old Dominion University

Original Publication Citation

Liao, S., & Wang, J. (2011). Stability analysis and application of a mathematical cholera model. *Mathematical Biosciences and Engineering*, *8*(3), 733-752. doi:10.3934/mbe.2011.8.733

MATHEMATICAL BIOSCIENCES
AND ENGINEERING
Volume **8**, Number **3**, July **2011**

doi:10.3934/mbe.2011.8.733

pp. **733–752**

STABILITY ANALYSIS AND APPLICATION OF A MATHEMATICAL CHOLERA MODEL

Shu Liao

School of Mathematics and Statistics
Chongqing Technology and Business University
Chongqing 400067, China

Jin Wang*

Department of Mathematics and Statistics
Old Dominion University
Norfolk, VA 23529, USA

(Communicated by Azmy Ackleh)

Abstract. In this paper, we conduct a dynamical analysis of the deterministic cholera model proposed in [9]. We study the stability of both the disease-free and endemic equilibria so as to explore the complex epidemic and endemic dynamics of the disease. We demonstrate a real-world application of this model by investigating the recent cholera outbreak in Zimbabwe. Meanwhile, we present numerical simulation results to verify the analytical predictions.

1. **Introduction.** Cholera, a water-borne disease caused by the bacterium *Vibrio cholerae*, continues to represent a significant public health burden in developing countries. For example, 142,311 cholera cases were officially reported in 2002 by 52 nations worldwide, among which Africa accounts for the majority. In 2006, the number of cholera cases climbed to almost 240,000 [42]. Mostly recently, the 2008-2009 cholera outbreak in Zimbabwe ended up with 98,592 reported cases and 4,288 deaths [40–42]. In addition, many believe the actual infection and death numbers have been far more than those reported due to poor surveillance and incomplete records.

Despite a large body of clinical, experimental and theoretical studies (see [1, 21, 25, 27, 29, 36] and the references therein), the fundamental mechanism of transmission for cholera is not well understood at present, which has hindered effective prevention and control strategies of the disease. The difficulty stems from the complex, multiple transmission pathways which include both direct human-to-human and indirect environment-to-human modes, and which distinct cholera from many other infectious diseases.

Mathematical modeling, simulation and analysis provide a promising way to look into the nature of the cholera dynamics, and many efforts have been devoted to this topic [3, 6, 9, 21, 29–31]. Among these, Capasso and Paveri-Fontana [3] proposed a

2000 *Mathematics Subject Classification.* Primary: 34D20, 92D30.
Key words and phrases. Stability, equilibrium, dynamical system, cholera model.
The second author is supported by NSF grant DMS-0813691.

simple deterministic model to study a cholera epidemic occurred in the Mediterranean in 1973. Codeço in 2001 published a model [6] that explicitly accounted for the environmental component, i.e., the *V. cholerae* concentration in the water supply, into a regular SIR epidemiological model. Hartley, Morris and Smith [9] in 2006 extended Codeço's work to include a hyperinfectious state of the pathogen, representing the "explosive" infectivity of freshly shed *V. cholerae*, based on the laboratory measurements that freshly shed *V. cholerae* from human intestines outcompeted other *V. cholerae* by as much as 700-fold for the first few hours in the environment [1, 25]. The article [9] provided deeper insight into cholera epidemics, though no rigorous dynamical analysis was presented in that work with its focus on medical aspects.

A goal of the present paper is to conduct a careful mathematical study on the cholera model of Hartley *et al.*, so as to explore the complex dynamics inherent in this model and to better understand the disease transmission mechanism. We will particularly study the stability property in both the epidemic and endemic dynamics through equilibrium analysis. For simple SI models with constant population, Lajmanovich and Yorke [18] proved that the disease-free equilibrium (DFE) is globally asymptotically stable when the basic reproduction number, R_0, is below 1; and when R_0 is above 1, there is a unique endemic equilibrium which is globally asymptotically stable. In other words, there is a stability exchange at $R_0 = 1$ in such models. Simon and Jacquez [33] extended this work and showed similar dynamics for a class of SI models with heterogeneous population. Meanwhile, several authors [5, 8, 32, 34] investigated more complicated dynamics, such as the backward bifurcation, of SI models for various infectious diseases. In addition, dynamical analysis of various SIR, SEI and SEIR models was conducted in [15–17, 24, 39], among others.

The model of Hartley *et al.*, differing from most epidemiological models, is a combination of a SIR formulation and two environmental variables, which lead to a combined human-environment epidemiological model and constitute a high-dimensional autonomous system (see equations 1-5). The stability analysis in the present paper shows that despite the incorporation of the environmental variables, there is a similar pattern of stability exchange at $R_0 = 1$. Specifically, we establish the following results for this cholera model: For $R_0 < 1$, there is a unique disease-free equilibrium which is both locally and globally asymptotically stable; this equilibrium becomes unstable when $R_0 > 1$. Meanwhile, there is a unique positive endemic equilibrium which is locally asymptotically stable when $R_0 > 1$. We will also briefly discuss the global asymptotic stability of the endemic equilibrium for a simplified, linear case. A complete study of the endemic global asymptotic stability for the full cholera model is challenging, and we plan to pursue it in a separate paper.

To verify our analysis and to demonstrate the application of this mathematical model, we apply it to investigate the 2008-2009 Zimbabwean cholera outbreak. Based on a sensitivity analysis with respect to the total infection, we fit the data by adjusting two key parameters in the model, i.e., the ingestion rates of hyperinfectious and non-hyperinfectious vibrios. We are able to conduct numerical simulations with various initial settings for sufficiently long time to reveal the endemic behavior of the disease. Our simulation results are consistent with the analytical predictions for both epidemic and endemic dynamics.

The remainder of this paper is organized as follows. In Section 2, we analyze the local and global stability of the disease-free equilibrium. This analysis naturally yields the basic reproduction number, R_0, which provides a sharp threshold for the epidemic dynamics. In Section 3, we study the endemic equilibrium with regard to the long-term dynamics of the disease. We prove the existence and local asymptotic stability of the positive endemic equilibrium when $R_0 > 1$, and briefly discuss its linear global asymptotic stability. In Section 4, we apply the model to investigate the Zimbabwean cholera outbreak and to verify our analytical results. Finally, we close the paper by some discussion in Section 5.

2. **The disease-free equilibrium.** The deterministic model of Hartley, Morris and Smith [9] consists of the following ordinary differential equations (ODE)

$$\frac{dS}{dt} = bN - \beta_L S\frac{B_L}{\kappa_L + B_L} - \beta_H S\frac{B_H}{\kappa_H + B_H} - bS \tag{1}$$

$$\frac{dI}{dt} = \beta_L S\frac{B_L}{\kappa_L + B_L} + \beta_H S\frac{B_H}{\kappa_H + B_H} - (\gamma + b)I \tag{2}$$

$$\frac{dR}{dt} = \gamma I - bR \tag{3}$$

$$\frac{dB_H}{dt} = \xi I - \chi B_H \tag{4}$$

$$\frac{dB_L}{dt} = \chi B_H - \delta_L B_L \tag{5}$$

Written in a vector form, the above equations become

$$\frac{d}{dt}X = \mathbf{F}(X) \tag{6}$$

with

$$X = \big(S,\ I,\ R,\ B_H,\ B_L\big)^T \tag{7}$$

Here S, I and R denote the susceptible, the infected, and the recovered numbers, respectively; $N = S + I + R$ is the total population which is assumed to be a constant. B_H and B_L denote the concentrations of the hyperinfectious (HI) and less-infectious (LI) vibrios. The parameters β_H and β_L represent the HI and LI ingestion rates, κ_H and κ_L the HI and LI half saturation rates (i.e., ID_{50}, the infectious dose sufficient to produce disease in 50% of those exposed), b the natural human birth/death rate, χ the bacterial transition rate, ξ the shedding rate, δ_L the bacterial death rate, and γ the recovery rate. To be biologically feasible, all these parameters are positive.

It is straightforward to see that equations (1-5) have a unique disease-free equilibrium (DFE)

$$X_0 = \big(N,\ 0,\ 0,\ 0,\ 0\big)^T \tag{8}$$

The local stability of the DFE, which is directly related to the disease epidemics [6, 12], is analyzed as follows.

The Jacobian of the ODE system (1-5) is

$$\begin{bmatrix} -\frac{\beta_L B_L}{\kappa_L+B_L} - \frac{\beta_H B_H}{\kappa_H+B_H} - b & 0 & 0 & -\beta_H S\frac{\kappa_H}{(\kappa_H+B_H)^2} & -\beta_L S\frac{\kappa_L}{(\kappa_L+B_L)^2} \\ \frac{\beta_L B_L}{\kappa_L+B_L} + \frac{\beta_H B_H}{\kappa_H+B_H} & -(\gamma+b) & 0 & \beta_H S\frac{\kappa_H}{(\kappa_H+B_H)^2} & \beta_L S\frac{\kappa_L}{(\kappa_L+B_L)^2} \\ 0 & \gamma & -b & 0 & 0 \\ 0 & \xi & 0 & -\chi & 0 \\ 0 & 0 & 0 & \chi & -\delta_L \end{bmatrix} \tag{9}$$

After substituting the values for the DFE: $S = N\,,\ I = R = B_H = B_L = 0\,,$ the above matrix becomes

$$J_B = \begin{bmatrix} -b & 0 & 0 & -\beta_H N\frac{1}{\kappa_H} & -\beta_L N\frac{1}{\kappa_L} \\ 0 & -(\gamma+b) & 0 & \beta_H N\frac{1}{\kappa_H} & \beta_L N\frac{1}{\kappa_L} \\ 0 & \gamma & -b & 0 & 0 \\ 0 & \xi & 0 & -\chi & 0 \\ 0 & 0 & 0 & \chi & -\delta_L \end{bmatrix}$$

The characteristic polynomial of the matrix J_B is found as

$$\begin{aligned} \mathrm{Det}\,(\lambda I - J_B) \;=\; & \Big[\lambda^3 + \lambda^2(\delta_L+\chi+\gamma+b) + \lambda\big(\chi\delta_L + \gamma\delta_L + \gamma\chi + b\delta_L + b\chi - \frac{\beta_H N\xi}{\kappa_H}\big) \\ & + \big(\gamma\chi\delta_L + b\chi\delta_L - \frac{\beta_H N\xi\delta_L}{\kappa_H} - \frac{\beta_L N\xi\chi}{\kappa_L}\big)\Big](\lambda+b)^2 \end{aligned}$$

The equilibrium (8) is locally asymptotically stable if and only if all roots of the above polynomial have negative real parts. Obviously $\lambda = -b$ is a negative root of multiplicity 2. To analyze the three roots of the cubic polynomial inside the square brackets, we set

$$\begin{aligned} b_1 &= \delta_L + \chi + \gamma + b \\ b_2 &= \chi\delta_L + \gamma\delta_L + \gamma\chi + b\delta_L + b\chi - \frac{\beta_H N\xi}{\kappa_H} \\ b_3 &= \chi\gamma\delta_L + b\chi\delta_L - \frac{\beta_H N\xi\delta_L}{\kappa_H} - \frac{\beta_L N\xi\chi}{\kappa_L} \end{aligned}$$

Based on the Routh-Hurwitz criterion [13,28], the sufficient and necessary condition for stability is

$$b_1 > 0\,, \qquad b_3 > 0\,, \qquad b_1\,b_2 - b_3 > 0 \tag{10}$$

Note that the first inequality is automatically satisfied since all the model parameters are positive. The second inequality, $b_3 > 0\,,$ holds if and only if

$$\big[-\chi(\gamma+b) + \frac{\beta_H N\xi}{\kappa_H}\big] + \frac{\beta_L N\xi\chi}{\kappa_L\delta_L} \;<\; 0 \tag{11}$$

which yields

$$N \;<\; \frac{(\gamma+b)\chi\kappa_H\kappa_L\delta_L}{\xi(\beta_H\kappa_L\delta_L + \beta_L\chi\kappa_H)} \tag{12}$$

In addition, we have

$$\begin{aligned} b_1b_2 - b_3 &= (\delta_L + \chi + \gamma + b)\big[\delta_L(\chi + \gamma + b) + \chi(\gamma + b) - \frac{\beta_H N\xi}{\kappa_H}\big] \\ &\quad - \gamma\chi\delta_L - b\chi\delta_L + \frac{\beta_H N\xi\delta_L}{\kappa_H} + \frac{\beta_L N\xi\chi}{\kappa_L} \\ &= (\chi + \gamma + b)[\delta_L(\delta_L + \chi + \gamma + b) + \chi(\gamma + b) - \frac{\beta_H N\xi}{\kappa_H}] + \frac{\beta_L N\xi\chi}{\kappa_L} \end{aligned}$$

It is thus clear to see that $b_1b_2 - b_3 > 0$ as long as the inequality (11) or, equivalently, (12), holds. The condition (12) provides a threshold for the total population (which is assumed to be completely susceptible initially):

$$S_c = \frac{(\gamma + b)\chi\kappa_H\kappa_L\delta_L}{\xi(\beta_H\kappa_L\delta_L + \beta_L\chi\kappa_H)} \tag{13}$$

When N is below S_c, the DFE is stable and no epidemicity would occur. In contrast, if N is above this critical value, the DFE becomes unstable and any infection entering the population would persist and lead to an epidemic.

We define the basic reproduction number, R_0, of this model by

$$R_0 = \frac{N}{S_c} = \frac{\xi(\beta_H\kappa_L\delta_L + \beta_L\chi\kappa_H)}{(\gamma + b)\chi\kappa_H\kappa_L\delta_L} N \tag{14}$$

Biologically speaking, R_0 represents the average number of secondary infections that occur when one infective is introduced into a completely susceptible host population [12, 37, 38]. The condition (12) is then equivalent to

$$R_0 < 1$$

Thus, we have established the result below

Theorem 2.1. *The disease-free equilibrium of the model (6) is locally asymptotically stable if $R_0 < 1$, and unstable if $R_0 > 1$.*

We mention that the basic reproduction number, given in equation (14), can also be derived by the next generation matrix analysis [37].

To study the global asymptotic stability of the DFE, one common approach is to construct an appropriate Lyapunov function [16, 18]). We have found, however, that it is simpler to apply the following result introduced by Castillo-Chavez *et al.* [4].

Lemma 2.2. [4] *Consider a model system written in the form*

$$\begin{aligned} \frac{dX_1}{dt} &= F(X_1, X_2), \\ \frac{dX_2}{dt} &= G(X_1, X_2), \qquad G(X_1, 0) = 0 \end{aligned} \tag{15}$$

where $X_1 \in \mathbb{R}^m$ denotes (its components) the number of uninfected individuals and $X_2 \in \mathbb{R}^n$ denotes (its components) the number of infected individuals including latent, infectious, etc; $X_0 = (X_1^*, 0)$ denotes the disease-free equilibrium of the system.

Also assume the conditions $(H1)$ and $(H2)$ below:
(H1) For $\frac{dX_1}{dt} = F(X_1, 0)$, X_1^* is globally asymptotically stable;
(H2) $G(X_1, X_2) = A\,X_2 - \hat{G}(X_1, X_2)$, $\hat{G}(X_1, X_2) \geq 0$ for $(X_1, X_2) \in \Omega$, where the Jacobian $A = \frac{\partial G}{\partial X_2}(X_1^*, 0)$ is an M-matrix (the off diagonal elements of A are nonnegative) and Ω is the region where the model makes biological sense.

Then the DFE $X_0 = (X_1^*, 0)$ *is globally asymptotically stable provided that* $R_0 < 1$.

Theorem 2.3. *The disease-free equilibrium of the model (6) is globally asymptotic stable if* $R_0 < 1$.

Proof. We only need to show that the conditions $(H1)$ and $(H2)$ hold when $R_0 < 1$. In our ODE system (1-5), $X_1 = (S,\, R)$, $X_2 = (I,\, B_H,\, B_L)$, and $X_1^* = (N,\, 0)$. We note that the system

$$\frac{dX_1}{dt} = F(X_1,\, 0) = \begin{bmatrix} bN - bS \\ \\ -bR \end{bmatrix}$$

is linear and its solution can be easily found as

$$R(t) = R(0)e^{-bt} \qquad \text{and} \qquad S(t) = N - \big(N - S(0)\big)\, e^{-bt}$$

Clearly, $R(t) \to 0$ and $S(t) \to N$ as $t \to \infty$, regardless of the values of $R(0)$ and $S(0)$. Thus $X_1^* = (N,\, 0)$ is globally asymptotically stable.

Next, we have

$$G(X_1,\, X_2) = \begin{bmatrix} \beta_L S \frac{B_L}{K_L + B_L} + \beta_H S \frac{B_H}{k_H + B_H} - (\gamma + b)I \\ \\ \xi I - \chi B_H \\ \\ \chi B_H - \delta_L B_L \end{bmatrix}$$

We can then obtain

$$A = \begin{bmatrix} -(\gamma + b) & \beta_H N \frac{1}{\kappa_H} & \beta_L N \frac{1}{\kappa_L} \\ \\ \xi & -\chi & 0 \\ \\ 0 & \chi & -\delta_L \end{bmatrix}$$

which is clearly an M-matrix. Meanwhile, we find

$$\hat{G}(X_1,\, X_2) = \left[\frac{\beta_H B_H \kappa_H (N - S) + \beta_H N B_H^2}{\kappa_H (\kappa_H + B_H)} + \frac{\beta_L B_L \kappa_L (N - S) + \beta_L N B_L^2}{\kappa_L (\kappa_L + B_L)} ,\quad 0 ,\quad 0 \right]^T$$

Since $0 \le S \le N$, it is obvious that $\hat{G}(X, Z) \ge 0$. □

3. Endemic dynamics.

3.1. Existence and local stability of endemic equilibrium.

The stability at the DEF determines the short-term epidemics of the disease, whereas its dynamics over a longer period of time is characterized by the stability at the endemic equilibrium. In this section we shall conduct the endemic analysis.

Let us denote the endemic equilibrium of system (6) by

$$X^* \;=\; \big(S^*,\, I^*,\, R^*,\, B_H^*,\, B_L^*\big)^T \tag{16}$$

Its components must satisfy

$$I^* = \frac{S^*}{\gamma+b}\left(\frac{\beta_L\xi I^*}{\delta_L\kappa_L+\xi I^*}+\frac{\beta_H\xi I^*}{\chi\kappa_H+\xi I^*}\right) \tag{17}$$

$$S^* = N-\frac{(\gamma+b)I^*}{b} \tag{18}$$

$$R^* = \frac{\gamma I^*}{b} \tag{19}$$

$$B_L^* = \frac{\xi I^*}{\delta_L} \tag{20}$$

$$B_H^* = \frac{\xi I^*}{\chi} \tag{21}$$

We first show the following theorem

Theorem 3.1. *The positive endemic equilibrium exists and is unique if and only if* $R_0>1$.

Proof. By manipulating equations (17-21), we obtain a cubic equation for I^*:

$$I^*\left[A(I^*)^2+BI^*+C\right]=0 \tag{22}$$

where

$$\begin{aligned} A &= -\xi^2(\gamma+b)(\beta_L+\beta_H+b)\\ B &= \xi^2bN(\beta_L+\beta_H)-\xi(\gamma+b)(\beta_L\chi\kappa_H+\beta_H\delta_L\kappa_L+b\delta_L\kappa_L+b\chi\kappa_H)\\ C &= \xi(\beta_L\chi\kappa_H+\beta_H\kappa_L\delta_L)(bN-bS_c) \end{aligned}$$

and where S_c is defined in equation (13). The zero root of equation (22) corresponds to the DFE. The other two (non-zero) roots, I_1 and I_2, of the equation must satisfy:

$$I_1I_2 = \frac{C}{A} \tag{23}$$

$$I_1+I_2 = -\frac{B}{A} \tag{24}$$

It is obvious that $A<0$ since all parameters are positive. When $R_0>1$, we have $N>S_c$ and $C>0$, so that the right-hand side of equation (23) is negative. Hence, there is one and only one positive real root for equation (22).

On the other hand, if $R_0<1$, then $N<S_c$ and $C<0$, so that the right-hand side of equation (23) is positive. Next we show $B<0$. We have

$$\xi^2bN(\beta_L+\beta_H)<\frac{\xi b(\beta_L+\beta_H)(\gamma+b)\chi\kappa_H\kappa_L\delta_L}{\beta_H\kappa_L\delta_L+\beta_L\chi\kappa_H} \tag{25}$$

when $N<S_c$ (see equation 13). Meanwhile,

$$b(\beta_L+\beta_H)(\gamma+b)\chi\kappa_H\kappa_L\delta_L<(\gamma+b)(\beta_L\chi\kappa_H+\beta_H\delta_L\kappa_L+b\delta_L\kappa_L+b\chi\kappa_H)(\beta_H\kappa_L\delta_L+\beta_L)$$

which yields

$$\frac{\xi b(\beta_L+\beta_H)(\gamma+b)\chi\kappa_H\kappa_L\delta_L}{\beta_H\kappa_L\delta_L+\beta_L\chi\kappa_H}<\xi(\gamma+b)(\beta_L\chi\kappa_H+\beta_H\delta_L\kappa_L+b\delta_L\kappa_L+b\chi\kappa_H) \tag{26}$$

Combining (25) and (26), we obtain $B<0$. Hence, the right-hand side of equation (24) is negative. In this case we either have two negative real roots, or two complex conjugate roots with negative real parts, for $A(I^*)^2+BI^*+C=0$. There is no positive endemic equilibrium.

Finally, if $R_0 = 1$, then $C = 0$ and equation (22) has only one nonzero root, $-\frac{B}{A}$, which is negative. □

We have the following result regarding the local stability of the endemic equilibrium.

Theorem 3.2. *When $R_0 > 1$, the positive endemic equilibrium of system (6) is locally asymptotically stable.*

Proof. Consider the Jacobian (9) at the endemic equilibrium. To make the algebraic manipulation simpler, we set

$$P = \beta_L \frac{B_L^*}{\kappa_L + B_L^*} + \beta_H \frac{B_H^*}{\kappa_H + B_H^*}, \quad Q = \beta_H S^* \frac{\kappa_H}{(\kappa_H + B_H^*)^2}, \quad T = \beta_L S^* \frac{\kappa_L}{(\kappa_L + B_L^*)^2} \tag{27}$$

Note that P, Q and T are all positive. The Jacobian matrix (9) then becomes

$$J_B^* = \begin{bmatrix} -P-b & 0 & 0 & -Q & -T \\ P & -(\gamma+b) & 0 & Q & T \\ 0 & \gamma & -b & 0 & 0 \\ 0 & \xi & 0 & -\chi & 0 \\ 0 & 0 & 0 & \chi & -\delta_L \end{bmatrix}$$

The characteristic polynomial of J_B^* is

$$\begin{aligned} \mathrm{Det}\,(\lambda I - J_B^*) &= (\lambda+b)\big[(\lambda+\delta_L)(\lambda+P+b)(\lambda+\gamma+b)(\lambda+\chi) \\ &\quad -\xi Q(\lambda+b)(\lambda+\delta_L) - T\xi\chi(\lambda+b)\big] \end{aligned}$$

Obviously, this equation has a negative root $\lambda = -b$. we expand the expression in the square brackets to obtain

$$a_4\lambda^4 + a_3\lambda^3 + a_2\lambda^2 + a_1\lambda^1 + a_0 = 0 \tag{28}$$

where

$$\begin{aligned} a_4 &= 1 \\ a_3 &= 2b + \chi + \delta_L + \gamma + P \\ a_2 &= b^2 + \gamma P + 2b\chi + 2b\delta_L + \chi\delta_L + b\gamma + \chi\gamma - Q\xi + \delta_L\gamma + bP + \chi P + \delta_L P \\ a_1 &= b^2\chi + b^2\delta_L + b\chi P + b\delta_L P + \chi\delta_L P + \chi\gamma P + \delta_L\gamma P + 2b\chi\delta_L + b\chi\gamma - Qb\xi \\ &\quad + b\delta_L\gamma + \chi\delta_L\gamma - Q\delta_L\xi - T\chi\xi \\ a_0 &= b^2\chi\delta_L + b\chi\delta_L\gamma - Qb\delta_L\xi - Tb\chi\xi + b\chi\delta_L P + \chi\delta_L\gamma P \end{aligned}$$

To ensure that all roots of equation (28) have negative real parts, the Routh-Hurwitz stability criterion [13] requires

$$a_3 > 0\,, \qquad a_1 > 0\,, \qquad a_0 > 0\,, \qquad a_1(a_2a_3 - a_1) > a_0a_3^2 \tag{29}$$

Among these $a_3 > 0$ is obvious. The other three inequalities in (29) hold when $R_0 > 1$; the details are provided in the Appendix. □

3.2. **Linear global stability.** The classical Poincaré-Bendixson theory [10] is a powerful tool to study global stability of nonlinear two-dimensional autonomous systems. However, this framework cannot be directly extended to higher-dimensional systems. Consequently, the global stability analysis of endemic equilibria for nonlinear higher-dimensional problems, such as the one in (1-5), is generally difficult, despite the efforts made by several authors [14–17,26,39]. For some special differential equation systems, one might be able to find a suitable Lyapunov function [18,20]

to prove the global stability. Unfortunately, there is no systematic way to construct or find Lyapunov functions, which hinders the application of this approach to more general model systems.

We speculate that the unique positive endemic equilibrium of system (1-5) is globally asymptotically stable when $R_0 > 1$. In the present paper, we will use a special linear case (see Case one below) to illustrate this point. We will also present numerical evidence (see Section 4) for nonlinear justification. It is our plan to rigorously investigate the global endemic stability of this model in another study.

Case one. We assume the pathogen concentrations in the environment are far beyond the HI and LI half saturation rates (ID_{50}), i.e., $B_L >> \kappa_L$ and $B_H >> \kappa_H$. Under this assumption, the incidence rates in the model become

$$\frac{B_L}{\kappa_L + B_L} \approx 1 \qquad \text{and} \qquad \frac{B_H}{\kappa_H + B_H} \approx 1$$

That is, the possibility of infection is about 100% to those exposed to pathogens. Since $R = N - I - S$, the model (1-5) is reduced to a two-dimensional linear system:

$$\frac{dS}{dt} = bN - (\beta + b)S \tag{30}$$

$$\frac{dI}{dt} = \beta S - (\gamma + b)I \tag{31}$$

with $\beta = \beta_L + \beta_H$. It is straightforward to determine the unique positive endemic equilibrium of this system:

$$S^* = \frac{bN}{\beta + b} \qquad \text{and} \qquad I^* = \frac{\beta bN}{(\beta + b)(\gamma + b)}$$

There is no DFE in this case for obvious reason. Meanwhile, the exact solution of the system (30, 31) can be quickly found as follows

$$S(t) = \frac{bN}{\beta + b} + \Big(S(0) - \frac{bN}{\beta + b}\Big)\, e^{-(\beta+b)t}$$

$$I(t) = \frac{\beta bN}{(\beta + b)(\gamma + b)} + C_1\, e^{-(\beta+b)t} + C_2\, e^{-(\gamma+b)t}$$

with

$$C_1 = \frac{\beta}{\gamma - \beta}\big(S(0) - \frac{bN}{\beta + b}\big), \qquad C_2 = I(0) - \frac{\beta bN}{(\beta + b)(\gamma + b)} - \frac{\beta}{\gamma - \beta}\big(S(0) - \frac{bN}{\beta + b}\big)$$

It is thus clear to see that $S(t) \to S^*$ and $I \to I^*$ as $t \to \infty$, regardless of the initial values of S and I. Hence, the endemic equilibrium $\big(S^*,\ I^*\big)$ is globally asymptotically stable.

This conclusion can also be easily obtained based on the famous Bendixson Theorem [10, 14], by noting that

$$\frac{\partial}{\partial S}\big(bN - (\beta + b)S\big) + \frac{\partial}{\partial I}\big(\beta S - (\gamma + b)I\big) = -(\gamma + 2b + \beta) < 0$$

holds everywhere, so that no periodic orbit can exist.

Case two. We now assume the pathogen concentrations are much lower than the half saturation rates, i.e., $B_L << \kappa_L$ and $B_H << \kappa_H$. Then we have

$$\frac{B_L}{\kappa_L + B_L} \approx 0 \qquad \text{and} \qquad \frac{B_H}{\kappa_H + B_H} \approx 0$$

which implies the chance of getting new infection is about 0. The model system (1-5) is then reduced to

$$\frac{dS}{dt} = bN - bS \tag{32}$$
$$\frac{dI}{dt} = -(\gamma + b)I \tag{33}$$

There is no endemic equilibrium in this case and the only equilibrium point of system (32, 33) is a DFE:

$$S_0 = N \qquad \text{and} \qquad I_0 = 0$$

The exact solution of equations (32) and (33) is

$$S(t) = N + (S(0) - N)e^{-bt}$$
$$I(t) = I(0)e^{-(\gamma+b)t}$$

Clearly, $S(t) \to S_0$ and $I(t) \to I_0$ as $t \to \infty$, confirming the global stability of the DFE (indeed, this is a special case of Theorem 2.3). The same conclusion can be obtained by using the Bendixson Theorem.

3.3. **Bifurcation diagram.** To summarize our stability analysis results, we sketch a bifurcation diagram [35] of I vs. R_0 for system (1-5) in Figure 1, which highlights the stability exchange at $R_0 = 1$ for the two biologically feasible equilibria: the DFE and the positive endemic equilibrium. To illustrate the positive endemic branch of the bifurcation, we write the endemic quadratic equation $A(I^*)^2 + BI^* + C = 0$ (see equation 22) as

$$A(I^*)^2 + (DR_0 - E)I^* + F(R_0 - 1) = 0 \tag{34}$$

where the constant coefficients D, E and F are given by

$$D = \xi^2 b S_c(\beta_L + \beta_h)$$
$$E = \xi(\gamma + b)(\beta_L \chi \kappa_H + \beta_H \delta_L \kappa_L) + b\xi(\gamma + b)(\delta_L \kappa_L + \chi \kappa_H)$$
$$F = bS_c\xi(\beta_L \chi \kappa_H + \beta_H \kappa_L \delta_L)$$

We then obtain

$$R_0 = 1 + \frac{-A(I^*)^2 + (E - D)I^*}{DI^* + F} \tag{35}$$

When I^* is small or moderate, equation (35) represents approximately a straight line passing the bifurcation point $R_0 = 1$, $I^* = 0$.

4. **A case study: the Zimbabwean cholera outbreak.** The 2008-2009 cholera outbreak in Zimbabwe was regarded as the worst African cholera epidemic in the last 15 years and received worldwide media attention [23, 40–42]. In order to improve our understanding of the development of this serious cholera outbreak, as well as for possible prediction and control of future cholera epidemics, we apply the mathematical model (1-5) to study the Zimbabwean cholera dynamics.

Among the many parameters in the model (1-5), κ_L, κ_H, χ, ξ, δ_L, γ have been estimated by various literatures [6, 11, 19, 25, 36]; their values are listed as follows and treated as reliable in the present paper: $\kappa_L = 10^6$ cells/ml, $\kappa_H = \kappa_L/700$, $\chi = (5\,\text{h})^{-1}$, $\xi = 10$ cells/ml $\cdot$ day, $\delta_L = (30\,\text{d})^{-1}$, $\gamma = (5\,\text{d})^{-1}$. Meanwhile, we take $b = (35\,\text{yr})^{-1}$ based on the life expectancy in Zimbabwe [41, 42].

In contrast, the values of β_L and β_H are less well known. The authors of [9] took $\beta_L = 1.5$/wk and β_H as a variable; they also stated that these two parameters are

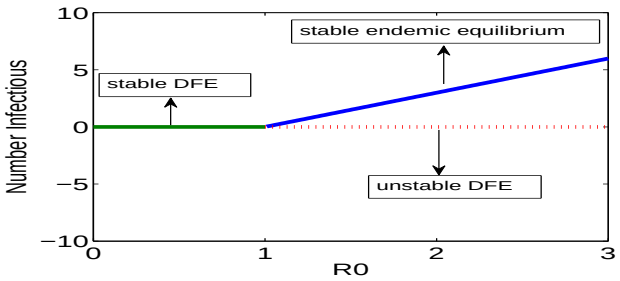

FIGURE 1. The bifurcation diagram of I vs. R_0 for the DFE and the positive endemic equilibrium. The solid lines represent the stable equilibria, and the dashed line represents the unstable equilibrium. There is a stability exchange at $R_0 = 1$. Biologically non-feasible equilibria are not shown on the diagram.

Parameters	Minimum	Maximum	PRCC values
β_L	0.01	3	0.245957
β_H	0.01	3	0.912184

TABLE 1. LHS sensitivity analysis for β_L and β_H with respect to the infection number I. The sample size is $n = 400$. Results show that the infection is especially sensitive to β_H.

particularly "difficult to estimate". This suggests that β_L and β_H are sensitive in the ODE model (1-5). To verify it, we have carried out a sensitivity analysis for these two parameters using the Latin Hypercube Sampling (LHS) method [2, 22]. The LHS method, which is one of the most efficient ways to analyze sensitivity and uncertainty, calculates the Partial Rank Correlation Coefficients (PRCC) in the range of $[-1, 1]$ for the model parameters with respect to outcome measurements. A small PRCC value (close to 0) indicates that changes in the input parameter have little impact on the outcome, whereas a bigger PRCC value suggests that the outcome is significantly influenced by, thus sensitive to, the changes of the input parameter. In this study we pick the total infection, I, as the outcome and present the results in Table 1 with a sample size $n = 400$; similar patterns are observed for differing sample sizes. The results confirm the sensitivity of the two parameters β_L and β_H; in particular, we observe that the number of the infected people is very sensitive to β_H.

In the work of [9], the ODE model (1-5) was introduced and discussed for a hypothetical community with a total population of $N = 10,000$. In order to assess the applicability of this model to the Zimbabwean cholera outbreak, we will first need to ensure the available Zimbabwean data can be reasonably fitted by the model results, which necessitates the adjustment of parameter values. The discussion in [9] and our sensitivity analysis indicate that the parameters β_L and β_H are sensitive and possibly vary from country to country. Hence, in what follows we adjust these two parameters to match the reported infections in Zimbabwe.

According to the published data by WHO [41, 42], the cholera outbreak started in the end of August 2008, with 11,735 cases reported by December 1, 2008, 79,613

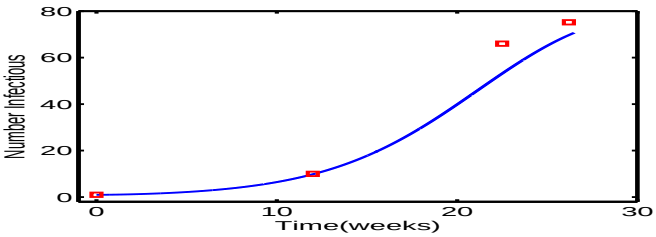

FIGURE 2. The data fitting for the infected population I, where the curve represents the model prediction and the squares mark the reported Zimbabwean data (normalized by a factor of 1,200).

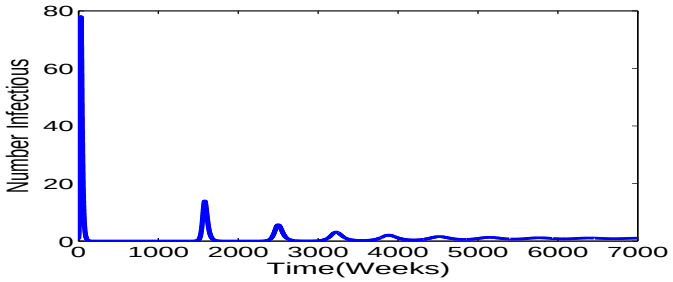

FIGURE 3. The infected population vs. time with the initial setting: $I(0) = 1,\ S(0) = 9999,\ R(0) = B_H(0) = B_L(0) = 0$. The curve exhibits several epidemic oscillations (outbreaks), then approaches the endemic equilibrium $I^* \doteq 0.9157$ after about 5,000 weeks.

cases by February 18, 2009 and 91,164 cases by March 17, 2009; afterwards the situation had improved significantly due to various control measures and international aids. Since the total population in Zimbabwe is about 12 million [42], we scale down this number by a factor of 1,200 to match the hypothetical population of $N = 10,000$ in [9]. Accordingly, we now have 10, 66 and 76 (normalized) cholera infections after 12 weeks, 22.5 weeks and 26.5 weeks, respectively, from the beginning of the outbreak. By varying the two parameters, we find that when $\beta_L = 0.126$ and $\beta_H = 0.0995$, the model prediction for the infected population, I, can well fit these data (see Figure 2).

By substituting the values of β_L, β_H and other parameters into equations (13) and (14), we find the basic reproduction number

$$R_0 \doteq 1.306$$

and the population threshold

$$S_c \doteq 7657$$

The fact that $R_0 > 1$ justifies the development of the cholera epidemics. The relatively low value of R_0 for the Zimbabwean cholera outbreak is attributed to the fact that although nearly 0.1 million cases have been reported, the overall percentage of infection with respect to the total population is still pretty low (less than 0.8%). The R_0 estimated here is regarded as a nationally averaged reproduction rate. Meanwhile, we substitute these parameter values into equations (22) and

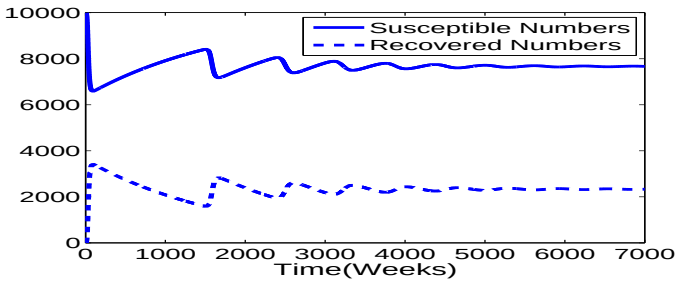

FIGURE 4. The susceptible and recovered populations vs. time with the initial setting: $I(0) = 1$, $S(0) = 9999$, $R(0) = B_H(0) = B_L(0) = 0$. Both curves exhibit several epidemic oscillations before approaching the endemic equilibrium: $S^* \doteq 7666$, $R^* \doteq 2333$.

(18-21), and find the unique positive endemic equilibrium:

$$S^* \doteq 7666, \qquad I^* \doteq 0.9157, \qquad R^* \doteq 2333, \qquad B_H^* \doteq 1.908, \qquad B_L^* \doteq 274.7$$

Note again that we have scaled down the total population in Zimbabwe by a factor of $1,200$ to match the hypothetical population $N = 10,000$. Thus, the model predicts that the realistic endemic infection number in Zimbabwe is about $1,099$.

To verify the model prediction, we run the numerical simulation for a much longer period of time (up to 7,000 weeks) and present the results for I, S and R in Figures 3 and 4. The first peak of the infection curve in Figure 3 represents the 2008-2009 cholera outbreak. The infection number (I) starts to decline once the susceptible population (S) falls below the threshold, $S_c \doteq 7657$. After this outbreak I drops to almost zero, meaning that the majority of the infected people have recovered and entered the R class, so that we see a significant increase of R in Figure 4. Then I stays at the zero level for the next 1,500 weeks or so (about 30 years). During this period R gradually decreases due to natural death of recovered individuals, whereas S gradually increases due to continuous birth of new susceptibles. Once the susceptible population exceeds the threshold S_c, another cholera outbreak is triggered but with much lower magnitude. This pattern continues for a few more outbreaks with decaying magnitudes. After about 5,000 weeks, the infection curve rests at the endemic value, $I^* \doteq 0.9157$; the S and R curves also converge to their endemic values, $S^* \doteq 7666$ and $R^* \doteq 2333$, respectively.

Figures 5 and 6 show the results of another numerical run with different initial conditions: $I(0) = 500$, $S(0) = 8500$, $R(0) = 1000$, $B_H(0) = B_L(0) = 0$. We observe very similar pattern. In particular, the I, S and R curves all approach their endemic equilibrium values after about 5,000 weeks. This pattern is also observed with various other initial conditions, which demonstrates the global asymptotic stability of the endemic equilibrium when $R_0 > 1$. Meanwhile, these results also justify the instability of the disease-free equilibrium, as cholera outbreaks occur whenever the susceptible population S exceeds the critical value S_c.

Finally, to validate the global asymptotical stability of the disease-free equilibrium when $R_0 < 1$, we have conducted many numerical runs with differing population N and initial conditions, and the results agree with the model prediction. A typical numerical result is presented in Figure 7, where the total hypothetical population is set as $N = 5,000$ (i.e., halving the current Zimbabwean population)

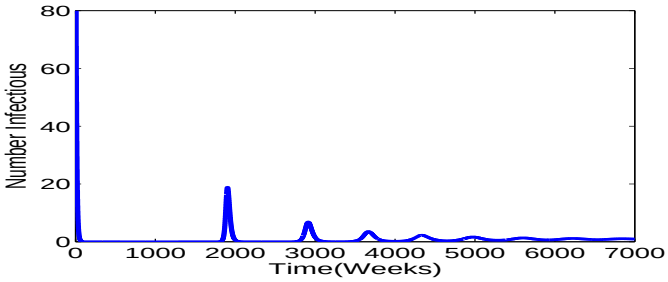

FIGURE 5. The infected population vs. time with the initial setting: $I(0) = 500,\ S(0) = 8500,\ R(0) = 1000,\ B_H(0) = B_L(0) = 0$. The curve exhibits several epidemic oscillations and then approaches the endemic equilibrium over time.

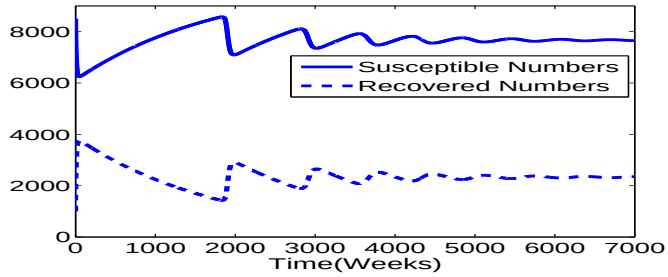

FIGURE 6. The susceptible and recovered populations vs. time with the initial setting: $I(0) = 500,\ S(0) = 8500,\ R(0) = 1000,\ B_H(0) = B_L(0) = 0$. Both curves exhibit several epidemic oscillations and then approach the endemic equilibrium over time.

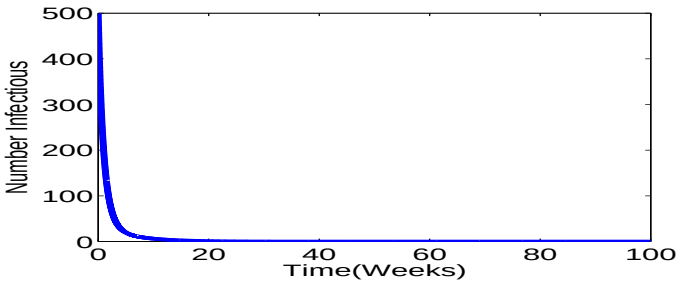

FIGURE 7. The infected population vs. time with the initial setting: $I(0) = 500,\ S(0) = 4500,\ R(0) = B_H(0) = B_L(0) = 0$. In this case $R_0 \doteq 0.653$ and the disease quickly dies out ($I = 0$).

so that $R_0 \doteq 0.653$. Initially I is 500; then the infection number quickly drops to zero and stays at zero for all time afterwards.

5. **Discussion.** We have conducted a stability analysis of the mathematical cholera model presented in equations (1-5), originally proposed by Hartley, Morris and

Smith [9]. We have studied the stability property at both the disease-free equilibrium (which determines the short-term epidemic behavior) and the endemic equilibrium (which determines the long-term disease dynamics). Our analysis shows a regular stability exchange at $R_0 = 1$ for this combined human-environment epidemiological model. To verify the analytical theory, we have performed numerical simulations and employed the most recent Zimbabwean cholera outbreak as a realistic case study. Our simulation results demonstrate that the model (1-5) is applicable to the cholera dynamics in Zimbabwe; the results for both epidemic and endemic dynamics are consistent with the analytical predictions.

The findings in this paper have several implications to the initiation and persistence of cholera infection. As mentioned before, one distinct feature of the model (1-5) is the incorporation of an hyperinfectious (H) state of the pathogen. Our sensitivity analysis shows that the number of infections is very sensitive to the parameter β_H. Together with the fact that the model can well fit the Zimbabwean data, our results support that the hyperinfectious state plays an important role in the transmission of the disease, especially for the onset of an epidemic. This point of view was carefully discussed in [9]. As pointed out in [30], the hyperinfectious state introduced in the model (1-5) can also be interpreted as a another way of modeling the direct human-to-human transmission. The model, when applied to Zimbabwean cholera, predicts that there will be a (smaller) cholera outbreak in every 20-30 years, and that the disease will remain endemic in the long term, unless there are significant changes to the current population and/or environment in Zimbabwe. We emphasize that this observation is purely based on the model system (1-5) and under the idealized condition that the population remains a constant for all the time. Thus it should be regarded as a model prediction under simplified settings, which, nonetheless, provides insight into the future evolution of cholera dynamics in this country. It is expected that similar studies can be performed to other cholera-endemic countries such as Mozambique, Zambia, and Bangladesh, with possible modifications of the model (e.g., adjustment of parameters).

The analysis and results presented in this work also enable us to study the control measures [7, 12] against cholera outbreak. For a simple illustration, we consider the use of vaccination and medical therapy (which could include hydration therapy, antibiotics, etc.) to control the disease. We assume that vaccination is introduced to the susceptible population at a rate of v, so that vS individuals per time are removed from the susceptible class and added to the recovered class. Similarly, we assume that medical therapy is applied to infected people at a rate of u, so that uI individuals per time are removed from the infected class and added to the recovered class. With the incorporation of these controls into the cholera model, equations (1-3) become

$$\frac{dS}{dt} = bN - \beta_L S\frac{B_L}{\kappa_L + B_L} - \beta_H S\frac{B_H}{\kappa_H + B_H} - bS - vS \tag{36}$$

$$\frac{dI}{dt} = \beta_L S\frac{B_L}{\kappa_L + B_L} + \beta_H S\frac{B_H}{\kappa_H + B_H} - (\gamma + b)I - uI \tag{37}$$

$$\frac{dR}{dt} = \gamma I - bR + vS + uI \tag{38}$$

whereas equations (4) and (5) remain the same. Conducting similar analysis as in Sec. 2 to this control model, we can easily obtain the (modified) basic reproduction

number:

$$R_0^c = \frac{\xi(\beta_H\kappa_L\delta_L + \beta_L\chi\kappa_H)}{\chi\kappa_H\kappa_L\delta_L}\,\frac{b\,N}{(b+v)(\gamma+b+u)} = \frac{b}{b+v}\,\frac{\gamma+b}{\gamma+b+u}\,R_0 \tag{39}$$

where R_0 is the basic reproduction number defined in equation (14) for the original model. Clearly $R_0^c < R_0$. The result in equation (39) shows that, mathematically, each of the two types of individual controls can reduce the value of R_0^c below 1 so that the disease will be eradicated. For example, if $v = 0$ (no vaccination), we would just need the rate of the medical therapy to be such that $u > (\gamma+b)(R_0-1)$ to ensure $R_0^c < 1$. Practically, however, the strength and the success of each control measure would be limited by social and economic factors and available resources, and the combination of different prevention and intervention approaches would possibly achieve the best result. Other types of control measures, such as sanitation, sewage treatment, and water cleaning, can be also incorporated into the model and the resulting values of R_0^c can be similarly calculated. Such information would provide useful guidelines for the public health administrations to effectively design disease control strategies and to properly scale their efforts.

There are a few limitations in this study. As mentioned before, the model (1-5) is based on the assumption that the natural birth and death rates are always equal. This may not be true in the real world, especially when a long period of time is concerned. Next, the disease-induced mortality is not included in the model. In fact, to our knowledge, none of the published mathematical cholera models (see, e.g., [3, 6, 9, 21, 29–31]) have considered this effect. This is perhaps due to the fact that most cholera infections are minor or moderate and can be effectively treated by simple hydration therapy; thus, in average, cholera-induced death rate is just about 1% [23, 42]. In contrast, the Zimbabwean cholera outbreak has a relatively high disease-caused death rate of 4.3% in average [23, 42]. It is thus expected that a model incorporating the disease mortality would yield more accurate results in modeling the Zimbabwean cholera. When the disease mortality is included and different natural birth and death rates are used, the total population N will vary in time. Specifically, it will be determined by the equation

$$\frac{dN}{dt} = (b_1 - b_2)\,N - \alpha I \tag{40}$$

where b_1 and b_2 denote the natural birth and death rates, respectively, and α denotes the disease mortality rate. The varying population size adds some complexity to the dynamical system, though, in principle, similar epidemic and endemic analysis can be conducted. Such models have been studied for several infectious diseases with regular SIR or SEIR formulations (see, e.g., [12, 16]). It is to be seen how the incorporation of the varying population size will change the dynamics of a combined human-environment epidemiological model system, particularly, the cholera model.

Acknowledgements. We would like to thank the two anonymous referees for their valuable comments to improve this paper.

Appendix. Based on Theorem 3.1, there is a unique positive endemic equilibrium when $R_0 > 1$. In what follows we show the last three inequalities in (29) at the endemic equilibrium.

First we rewrite a_0 as

$$a_0 = P(\gamma+b)\chi\delta_L + b(\gamma+b)\chi\delta_L - b\xi(\chi T + \delta_L Q) \tag{41}$$

Substituting equations (20) and (21) into (17) and (18), we obtain

$$\gamma + b = \xi S^*\left(\frac{\beta_L}{\kappa_L\delta_L + \xi I^*} + \frac{\beta_H}{\chi\kappa_H + \xi I^*}\right) \tag{42}$$

Using equations (27) and (42), we have

$$\begin{aligned} a_0 &= P(\gamma+b)\chi\delta_L + b\xi\chi\delta_L S^*\left[\frac{\beta_L}{\kappa_L\delta_L + \xi I^*} + \frac{\beta_H}{\chi\kappa_H + \xi I^*}\right] \\ &\quad - b\xi\chi\delta_L S^*\left[\frac{\beta_L\delta_L\kappa_L}{(\kappa_L\delta_L + \xi I^*)^2} + \frac{\beta_H\chi\kappa_H}{(\chi\kappa_H + \xi I^*)^2}\right] \\ &= P(\gamma+b)\chi\delta_L + b\xi\chi\delta_L S^*\left[\frac{\beta_L\xi I^*}{(\kappa_L\delta_L + \xi I^*)^2} + \frac{\beta_H\xi I^*}{(\chi\kappa_H + \xi I^*)^2}\right] \\ &> 0 \end{aligned}$$

Next, we rewrite a_1 into the sum of three parts:

$$\begin{aligned} a_1 &= (b^2\chi + b\gamma\chi - Qb\xi) + (\delta_L\chi\gamma + \delta_L\chi b - Q\delta_L\xi - T\chi\xi) \\ &\quad + (b\chi P + b\delta_L P + \chi\delta_L P + \chi\gamma P + \delta_L\gamma P + b\chi\delta_L + b\delta_L\gamma) \end{aligned} \tag{43}$$

Note that the last part in equation (43) is positive. After substitution of equations (27) and (42), the first two parts of a_1 become

$$\begin{aligned} b^2\chi + b\gamma\chi - Qb\xi &= \xi b\chi S^*\left(\frac{\beta_L}{\kappa_L\delta_L + \xi I^*} + \frac{\beta_H}{\chi\kappa_H + \xi I^*}\right) - \xi b\beta_H S^*\frac{\kappa_H}{(\kappa_H + \frac{\xi I^*}{\chi})^2} \\ &= \xi b\chi S^*\left[\frac{\beta_L}{\kappa_L\delta_L + \xi I^*} + \frac{\beta_H}{\chi\kappa_H + \xi I^*} - \frac{\beta_H\kappa_H\chi}{(\kappa_H\chi + \xi I^*)^2}\right] \\ &= \xi b\chi S^*\left[\frac{\beta_L}{\kappa_L\delta_L + \xi I^*} + \frac{\beta_H\xi I^*}{(\kappa_H\chi + \xi I^*)^2}\right] \\ &> 0 \end{aligned}$$

and

$$\begin{aligned} &\delta_L\chi\gamma + \delta_L\chi b - Q\delta_L\xi - T\chi\xi \\ &= \xi\delta_L\chi S^*\left(\frac{\beta_L}{\kappa_L\delta_L + \xi I^*} + \frac{\beta_H}{\chi\kappa_H + \xi I^*}\right) - \xi\left[\chi\beta_L S^*\frac{\kappa_L}{(\kappa_L + \frac{\xi I^*}{\delta_L})^2} + \delta_L\beta_H S^*\frac{\kappa_H}{(\kappa_H + \frac{\xi I^*}{\chi})^2}\right] \\ &= \xi\delta_L\chi S^*\left[\frac{\beta_L}{\kappa_L\delta_L + \xi I^*} + \frac{\beta_H}{\chi\kappa_H + \xi I^*} - \frac{\beta_L\kappa_L\delta_L}{(\kappa_L\delta_L + \xi I^*)^2} - \frac{\beta_H\kappa_H\chi}{(\kappa_H\chi + \xi I^*)^2}\right] \\ &= \xi\delta_L\chi S^*\left[\frac{\beta_L\xi I^*}{(\kappa_L\delta_L + \xi I^*)^2} + \frac{\beta_H\xi I^*}{(\kappa_H\chi + \xi I^*)^2}\right] \\ &> 0 \end{aligned}$$

Thus $a_1 > 0$ holds.

To prove the last inequality in (29), i.e., $a_1a_2a_3 - a_1^2 > a_0a_3^2$, it is sufficient to establish the following two inequalities:

$$a_1a_2a_3 > 2a_1^2 \tag{44}$$

$$a_1a_2a_3 > 2a_0a_3^2 \tag{45}$$

To show (44), we write $a_2a_3 - 2a_1$ into the sum of four parts:

$$\begin{aligned} a_2a_3 - 2a_1 &= (P\chi b + P\chi\gamma - PQ\xi) + (\chi^2 b + \chi^2\gamma - Q\chi\xi) + (\chi b^2 + \chi\gamma^2 + 2b\gamma\chi - Q\gamma\xi) \\ &\quad + \big(3Pb^2 + P^2 b + P\chi^2 + P^2\chi + P\delta_L^2 + P^2\delta_L + P\gamma^2 + P^2\gamma + b\chi^2 + 2b^2\chi \\ &\quad + 2b\delta_L^2 + 3b^2\delta_L + \chi\delta_L^2 + \chi^2\delta_L + b\gamma^2 + 3b^2\gamma + \delta_L\gamma^2 + \delta_L^2\gamma + 2b^3 + 2Pb\chi \\ &\quad + 3Pb\delta_L + P\chi\delta_L + 4Pb\gamma + P\delta_L\gamma + 2b\chi\delta_L + b\chi\gamma + 3b\delta_L\gamma + \chi\delta_L\gamma \\ &\quad + Q\delta_L\xi + 2T\chi\zeta\big) \end{aligned}$$

Note again that the last part in the above expression is positive. After substitution of equations (27) and (42), the first part becomes

$$\begin{aligned} P\chi b + P\chi\gamma - PQ\xi &= P\Big[\xi\chi S^*\big(\frac{\beta_L}{\kappa_L\delta_L + \xi I^*} + \frac{\beta_H}{\chi\kappa_H + \xi I^*}\big) - \xi\beta_H S^* \frac{\kappa_H}{(\kappa_H + B_H)^2}\Big] \\ &= P\xi\chi S^*\Big[\frac{\beta_L}{\kappa_L\delta_L + \xi I^*} + \frac{\beta_H}{\chi\kappa_H + \xi I^*} - \frac{\beta_H\kappa_H\chi}{(\kappa_H\chi + \xi I^*)^2}\Big] \\ &= P\xi\chi S^*\Big[\frac{\beta_L}{\kappa_L\delta_L + \xi I^*} + \frac{\beta_H\xi I^*}{(\kappa_H\chi + \xi I^*)^2}\Big] \\ &> 0 \end{aligned} \tag{46}$$

In a similar way, we can prove $\chi^2 b + \chi^2\gamma - Q\chi\xi > 0$ and $\chi b^2 + \chi\gamma^2 + 2b\gamma\chi - Q\gamma\xi > 0$. Thus (44) holds.

Finally, to show (45), we write $a_1a_2 - 2a_0a_3$ into the sum of many parts as follows:

$$\begin{aligned} a_1a_2 - 2a_0a_3 &= (Pb\chi\delta_L^2 + P\chi\delta_L^2\gamma - TP\chi\delta_L\xi - PQ\delta_L^2\xi) + (\chi\delta_L^2\gamma^2 + b\chi\delta_L^2\gamma - T\chi\delta_L\gamma\xi - Q\delta_L^2\gamma\xi) \\ &\quad + (P^2\chi^2\delta_L - T\chi^2\gamma\xi - Q\chi\delta_L\gamma\xi) + (b^4\chi + b^3\chi\gamma - Qb^3\xi) \\ &\quad + (b^3\chi\gamma + b^2\chi\delta_L\gamma + b^2\chi\gamma^2 + b\chi\delta_L\gamma^2 - Qb^2\gamma\xi - Qb\delta_L\gamma\xi) \\ &\quad + (Pb^3\chi + Pb\chi\gamma^2 + 2Pb^2\chi\gamma - PQb^2\xi - PQb\gamma\xi) \\ &\quad + (3b^2\chi^2\delta_L + 3b\chi^2\delta_L\gamma - 3Qb\chi\delta_L\xi) + (2Pb^2\chi^2 + 2Pb\chi^2\gamma - 2PQb\chi\xi) \\ &\quad + (P\chi^2\delta_L^2 + P\chi^2\gamma^2 + P\chi^2\delta_L b - PQ\chi\delta_L\xi) + (Pb^2\chi^2 + 2b^3\chi^2 + 3b^2\chi^2\gamma - 3Qb^2\chi\xi) \\ &\quad + (P\chi^2\delta_L\gamma + P\chi^2\delta_L b - TP\chi^2\xi - PQ\chi\delta_L\xi) + (2Pb\chi^2\gamma - 2Qb\chi\gamma\xi) \\ &\quad + (P\chi\gamma^2\delta_L + P\chi b\delta_L\gamma - TP\chi\gamma\xi - PQ\delta_L\gamma\xi) + (P^2\chi^2\gamma - PQ\chi\gamma\xi) \\ &\quad + (Pb^2\chi\delta_L + Pb\chi\delta_L\gamma - PQb\delta_L\xi) + (\delta_L^2\chi^2\gamma + \delta_L^2\chi^2 b - T\chi^2\delta_L\xi - Q\chi\delta_L^2\xi) \\ &\quad + (\chi^2\delta_L\gamma^2 + \chi^2\delta_L^2 b + \chi^2 b\gamma^2 - Q\chi\delta_L\gamma\xi) + (P^2\chi\gamma\delta_L - PQ\delta_L\gamma\xi) \\ &\quad + P^2b^2\chi + P^2b^2\delta_L + P^2b\chi^2 + P^2b\chi\delta_L + 2P^2b\chi\gamma + P^2b\delta_L^2 + 2P^2b\delta_L\gamma \\ &\quad + P^2\chi\delta_L^2 + P^2\chi\gamma^2 + P^2\delta_L^2\gamma + P^2\delta_L\gamma^2 + Pb^3\chi + 2Pb^3\delta_L + 2Pb^2\chi\delta_L \\ &\quad + 2Pb^2\chi\gamma + 3Pb^2\delta_L^2 + 4Pb^2\delta_L\gamma + Pb\chi^2\delta_L + 2Pb\chi\delta_L^2 + 2Pb\chi\delta_L\gamma + Pb\chi\gamma^2 \\ &\quad + TPb\chi\xi + 4Pb\delta_L^2\gamma + 2Pb\delta_L\gamma^2 + P\delta_L^2\gamma^2 + Q^2b\xi^2 + Q^2\delta_L\xi^2 + TQ\chi\xi^2 + b^4\delta_L \\ &\quad + 2b^3\chi\delta_L + 2b^3\delta_L^2 + 2b^3\delta_L\gamma + 3b^2\chi\delta_L^2 + 2b^2\chi\delta_L\gamma + 3Tb^2\chi\xi \\ &\quad + 3b^2\delta_L^2\gamma + b^2\delta_L\gamma^2 + 2b\chi\delta_L^2\gamma + Tb\chi\gamma\xi + b\delta_L^2\gamma^2 \end{aligned}$$

Equations (27) and (42) are again used in the term-by-term manipulation of the long expression above, to establish $a_1a_2 - 2a_0a_3 > 0$.

REFERENCES

[1] A. Alam, R. C. Larocque, J. B. Harris, et al., *Hyperinfectivity of human-passaged Vibrio cholerae can be modeled by growth in the infant mouse*, Infection and Immunity, **73** (2005), 6674–6679.

[2] S. M. Blower and H. Dowlatabadi, *Sensitivity and uncertainty analysis of complex models of disease transmission: An HIV model, as an example*, International Statistical Review, **62** (1994), 229–243.

[3] V. Capasso and S. L. Paveri-Fontana, *A mathematical model for the 1973 cholera epidemic in the european mediterranean region,* Revue Dépidémoligié et de Santé Publiqué, **27** (1979), 121–132.
[4] C. Castillo-Chavez, Z. Feng and W. Huang, *On the computation of R_0 and its role on global stability*, in "Mathematical Approaches for Emerging and Reemerging Infectious Diseases: An Introduction," IMA, **125**, Springer-Verlag, 2002.
[5] N. Chitnis, J. M. Cushing and J. M. Hyman, *Bifurcation analysis of a mathematical model for malaria transmission*, SIAM Journal on Applied Mathematics, **67** (2006), 24–45.
[6] C. T. Codeço, *Endemic and epidemic dynamics of cholera: The role of the aquatic reservoir,* BMC Infectious Diseases, **1**, 2001.
[7] K. Dietz, *The estimation of the basic reproduction number for infections diseases*, Statistical Methods in Medical Research, **2** (1993), 23–41.
[8] J. Dushoff, W. Huang and C. Castillo-Chavez, *Backwards bifurcation and catastrophe in simple models of fatal diseases*, Journal of Mathematical Biology, **36** (1998), 227–248.
[9] D. M. Hartley, J. G. Morris and D. L. Smith, *Hyperinfectivity: A critical element in the ability of V. cholerae to cause epidemics?*, PLoS Medicine, **3** (2006), 63–69.
[10] P. Hartman, "Ordinary Differential Equations," John Wiley, New York, 1980.
[11] T. R. Hendrix, *The pathophysiology of cholera*, Bulletin of the New York Academy of Medicine, **47** (1971), 1169–1180.
[12] H. W. Hethcote, *The mathematics of infectious diseases,* SIAM Review, **42** (2000), 599–653.
[13] G. A. Korn and T. M. Korn, "Mathematical Handbook for Scientists and Engineers: Definitions, Theorems, and Formulas for References and Review," Dover Publications, Mineola, NY, 2000.
[14] B. Li, *Periodic orbits of autonomous ordinary differential equations: Theory and applications,* Nonlinear Analysis, **5** (1981), 931–958.
[15] G. Li and J. Zhen, *Global stability of an SEI epidemic model with general contact rate*, Chaos Solitons Fractals, **23** (2005), 997–1004.
[16] M. Y. Li, J. R. Graef, L. Wang and J. Karsai, *Global dynamics of a SEIR model with varying total population size*, Mathematical Biosciences, **160** (1999), 191–213.
[17] M. Y. Li and J. S. Muldowney, *Global stability for the SEIR model in epidemiology,* Mathematical Biosciences, **125** (1995), 155–164.
[18] A. Lajmanovich and J. Yorke, *A deterministic model for gonorrhea in a nonhomogeneous population*, Mathematical Biosciences, **28** (1976), 221–236.
[19] J. B. Kaper, J. G. Morris and M. M. Levine, *Cholera*, Clinical Microbiology Reviews **8** (1995), 48–86.
[20] H. K. Khalil, "Nonlinear Systems," Prentice Hall, NJ, 1996.
[21] A. A. King, E. L. Lonides, M. Pascual and M. J. Bouma, *Inapparent infections and cholera dynamics*, Nature, **454** (2008), 877–881.
[22] S. Marino, I. Hogue, C. J. Ray and D. E. Kirschner, *A methodology for performing global uncertainty and sensitivity analysis in system biology,* Journal of Theoretical Biology, **254** (2008), 178–196.
[23] P. R. Mason, *Zimbabwe experiences the worst epidemic of cholera in Africa*, Journal of Infection in Developing Countries, **3** (2009), 148–151.
[24] J. Mena-Lorca and H. W. Hethcote, *Dynamic models of infectious diseases as regulator of population sizes,* Journal of Mathematical Biology, **30** (1992), 693–716.
[25] D. S. Merrell, S. M. Butler, F. Qadri, et al., *Host-induced epidemic spread of the cholera bacterium*, Nature, **417** (2002), 642–645.
[26] S. M. Moghadas and A. B. Gumel, *Global stability of a two-stage epidemic model with generalized non-linear incidence*, Mathematics and Computers in Simulation, **60** (2002), 107–118.
[27] E. J. Nelson, J. B. Harris, J. G. Morris, S. B. Calderwood and A. Camilli, *Cholera transmission: The host, pathogen and bacteriophage dynamics*, Nature Reviews: Microbiology, **7** (2009), 693–702.
[28] R. M. Nisbet and W. S. C. Gurney, "Modeling Fluctuating Populations," John Wiley & Sons, New York, 1982.
[29] M. Pascual, M. Bouma and A. Dobson, *Cholera and climate: Revisiting the quantiative evidence,* Microbes and Infections, **4** (2002), 237–245.
[30] M. Pascual, K. Koelle and A. Dobson, *Hyperinfectivity in cholera: A new mechanism for an old epidemiological model?*, PLoS Medicine, **3** (2006), 931–933.

[31] E. Pourabbas, A. d'Onofrio and M. Rafanelli, *A method to estimate the incidence of communicable diseases under seasonal fluctuations with application to cholera,* Applied Mathematics and Computation, **118** (2001), 161–174.
[32] T. C. Reluga, J. Medlock and A. S. Perelson, *Backward bifurcation and multiple equilibria in epidemic models with structured immunity,* Journal of Theoretical Biology, **252** (2008), 155–165.
[33] C. P. Simon and J. A. Jacquez, *Reproduction numbers and the stability of equilibria of SI models for heterogeneous populations*, SIAM Journal on Applied Mathematics, **52** (1992), 541–576.
[34] B. H. Singer and D. Kirschner, *Influence of backward bifurcation on interpretation of R_0 in a model of epidemic tuberculosis with reinfection,* Mathematical Biosiences and Engineering, **1** (2004), 91–93.
[35] D. Terman, *An introduction to dynamical systems and neuronal dynamics,* in "Tutorials in Mathematical Biosciences I," Springer, Berlin/Heidelberg, 2005.
[36] V. Tudor and I. Strati, "Smallpox, Cholera," Tunbridge Wells: Abacus Press, 1977.
[37] P. van den Driessche and J. Watmough, *Reproduction numbers and sub-threshold endemic equilibria for compartmental models of disease transmission,* Mathematical Biosciences, **180** (2002), 29–48.
[38] E. Vynnycky, A. Trindall and P. Mangtani, *Estimates of the reproduction numbers of spanish influenza using morbidity data,* International Journal of Epidemiology, **36** (2007), 881–889.
[39] J. Zhang and Z. Ma, *Global dynamics of an SEIR epidemic model with saturating contact rate,* Mathematical Biosciences, **185** (2003), 15–32.
[40] Center for Disease Control and Prevention, Available from: http://www.cdc.gov.
[41] The Wikipedia, Available from: http://en.wikipedia.org.
[42] World Health Organization, Available from: http://www.who.org.

Received July 1, 2010; Accepted September 22, 2010.

E-mail address: sliao002@odu.edu
E-mail address: j3wang@odu.edu